Available online at www.sciencedirect.com

ScienceDirect

Ceramics International 40 (2014) 2073–2081

CERAMICS INTERNATIONAL

www.elsevier.com/locate/ceramint

Wettability of 2519Al on B_4C at 1000–1250 °C and mechanical properties of infiltrated B_4C–2519Al composites

Haobo Wu, Fanhao Zeng*, Tiechui Yuan, Fuqin Zhang, Xiang Xiong

State Key Laboratory of Powder Metallurgy, Powder Metallurgy Research Institute, Central South University, Changsha 410083, China

Received 21 February 2013; received in revised form 25 July 2013; accepted 25 July 2013
Available online 1 August 2013

Abstract

The wettability of 2519Al on boron carbide (B_4C) was investigated in detail by an improved sessile-drop method at temperature ranging from 1000 to 1250 °C. The interface reactions of B_4C–2519Al systems were analyzed by means of scanning electron microscopy (SEM), electron probe X-Ray microanalysis (EPMA) and X-ray diffraction (XRD). Typical flexural strength and hardness of infiltrated B_4C–2519Al composites were studied by three-point-bending tests and Rockwell hardness tester. It is found that the wettability and interaction between molten 2519Al alloy and B_4C are sensitive to the temperature and contact time. The contact angles significantly decreased and the solid–liquid interaction was more intense as the temperature increased. On the other hand, the formation of various compounds such as Al_3BC, $Al_3B_{48}C_2$ and AlB_2 was identified. Some Al_2Cu and Al_3Zr phases appeared in the 2519Al drop during cooling, while AlB_2 precipitated far away from the 2519Al/B_4C interface. Ternary compounds of Al_3BC and $Al_3B_{48}C_2$, formed along the interface, play a key role in the improvement of wettability of B_4C/2519Al. For infiltrated 2519Al–B_4C composites, the typical bending strength and HRA are 300.71 MPa and 80.3, respectively. The main fracture way of infiltrated B_4C/2519Al is transgranular rupture, which has smooth fracture surface and intrinsic brittle fracture mode.

Keywords: C. Mechanical properties; Wetting; Contact angle; EPMA

1. Introduction

Boron carbide (B_4C) has a low density (2.52 g/cm^3), a high hardness chemical potential, and high capacity for absorbing thermal neutron. Due to the outstanding properties, B_4C ceramics have great potential for many applications such as neutron absorber, blasting nozzles and especially light ceramic armor [1,2]. However, due to the strong covalent bonds, densification of stoichiometric boron carbide (B_4C) is extremely difficult. Moreover, the fracture toughness of B_4C ceramic is about 3.7 MPa m$^{1/2}$, which limited its applications in industrial applications [3].

It has been known that combining B_4C with a metal such as Al to B_4C–metal composites could improve the toughness of B_4C ceramic. B_4C–Al composites have the potential for offering a combination of high hardness and better toughness in a lightweight structure. There are several methods to fabricate the B_4C–Al composites or cermets, including powder metallurgy, hot-press and pressureless infiltration. Among these methods, pressureless infiltration method, namely, infiltration molten Al into porous B_4C preforms under an inert atmosphere has been of more interest as a cost-effective method [4].

In the infiltration process of compositing, the feasibility for preparing materials and the performance of materials are largely determined by wetting behavior of molten aluminum on B_4C. Halverson [5] measured the contact angles of pure Al on B_4C based on sessile drops, finding that their contact angles at 1000 °C in the first 10min ranged from 104° to 80°. Naidich [6] reported that the contact angle of Al–B_4C is as high as 147° at 1000 °C, while it decreased sharply with increase in temperature and a value of 33° was obtained at 1150 °C after an isothermal dwell for 5min. Panasyuk [7] investigated the wetting kinetics of molten Al on the B_4C surfaces at 1100–1200 °C. It was found that their contact angle was initially 92° and then decreased to 28° in 3–5 min and the wetting was assumed to associate with the formation of an unknown compound in the contact zone. By using an improved sessile-drop method, Qiaoli Lin [8] reported that the contact angle of pure Al on boron carbide substrate are initially 56°

*Corresponding author. Tel.: +86 731 88877880; fax: +86 731 88710855.
E-mail address: zengfanhao608@csu.edu.cn (F. Zeng).

0272-8842/$ - see front matter © 2013 Elsevier Ltd and Techna Group S.r.l. All rights reserved.
http://dx.doi.org/10.1016/j.ceramint.2013.07.120

and then decreased to 4° in 100 s at 1200 °C. For Al alloys on B_4C, Frage [9] investigated the effects of Al content in the Cu–Al and Sn–Al alloy on the wetting behavior of B_4C/(Me–Al) systems, indicating that the wetting behavior is governed by the thermodynamic properties of the binary liquid system. On the other hand, the chemical reactivity of hot-pressed B_4C–Al was studied at temperatures ranging from 627 °C to 1000 °C [10]. It showed that at 868 °C, the reaction products are Al_3BC and AlB_2. At temperatures higher than 868 °C, Al_3BC is still formed while $Al_3B_{48}C_2$ replaces some AlB_2. However, Lee [11] and Arslan [12] considered that other phases, such as AlB_{12} ($Al_3B_{48}C_2$), AlB_{10} ($AlB_{24}C_4$), $AlB_{12}C_2$ and Al_4C_3, can be formed in B_4C/Al composites, depending on the reaction temperature.

Compared to hot-pressed boron carbide, the hardness of B_4C–Al composites decreased because some relatively soft Al exists in the composites. In order to improve the hardness of the composites, Al alloy is a good choice to substitute pure Al as binder metal because of their hot treatment hardening effects. 2519Al (Al–5.8,Cu–0.3,Mn–0.2,Mg–0.2,Zr, mass fraction %) is a hard aluminum, which has been used as functionally graded armor plate [13,14]. Nevertheless, the wettability of 2519Al on B_4C has not been reported so far. In this study, the B_4C substrates were fabricated by the hot-press method, and the wetting behavior and interface reactions of B_4C/2519Al at temperatures from 1000–1250 °C were investigated using a modified sessile-drop method [15]. Moreover, the typical mechanical properties of B_4C–2519Al composites were studied. It showed that the wettability and interactions between 2519Al and B_4C were sensitive to the temperature and contact time. The contact angle significantly decreased and the solid–liquid interactions were more intense as the temperature increased.

2. Experimental

The B_4C substrates were prepared by hot pressing fine pure powder under inert atmosphere at 1800 °C and then pressureless sintering at 2100 °C. The boron carbide powders (average grain size of 5 μm) were milled and mixed in a planetary mill in methanol for 1 h using high-purity tungsten carbide balls. After drying at 100 °C, the powder mixtures were uniaxially cold pressed under 120 MPa into 50-mm inner diameter and 30-mm inner height samples in stainless steel mold. Green compacts were then hot-pressed in 50-mm diameter cylindrical double action graphite dies at 1800 °C under 20 MPa using HI-MVLTI-10000 graphite element furnace. Hot pressing sintering and heat treatment were carried out under Ar atmosphere using a heating rate of 10 °C/min. The sintered boron carbide bodies were cut to plate of Φ20 mm × 10 mm, surface ground on diamond disc and polished with diamond paste with the size of 5 μm and 2.5 μm, respectively. For optical microstructure examination, the polished surfaces were electrochemically etched in a 1% KOH solution with a current density of 0.03 A/cm^2 for 60–120 s [16,17].

The 2519Al sheets were prepared by starting materials of Al–50Cu, Al–Mn, Al–Zr and pure Mg. The alloys were melted in a resistance furnace at 780 °C and casting at 730 °C in an iron die. After 525 °C × 1 h solid solution treatment, the casting ingots were cold rolled and then aged at 165 °C for 16 h. Before wetting experiment, the 2519Al sheets were cut to what the experiment required, and the sheets were then ultrasonically cleaned in acetone.

An improved sessile-drop method which was called a dispensed sessile drop method, as described in detail elsewhere [15], was employed for the wetting experiments. In this method, the sessile drop was formed by extruding through a narrow orifice (1 mm diameter) of an alumina tube and dropping onto the substrate surface. In this case, the initial oxide on the Al surface can be mechanically removed and the measured contact angles are more accurate and closer to the true contact angles of the 2519Al/B_4C system. The main advantages of this modified method lie in that it enables the isothermal spreading kinetics to be fully monitored and that it eliminates the pre-interaction of the molten alloy with the substrate. The process of this experiment was to put the molten 2519A alloy on Al_2O_3 extrusion pipe of the experimental device initially, then vacuum the device, and then heated to the set temperature. A drop of alloy dripped on the substrate from the opening seized 1 mm on the front of Al_2O_3 extrusion pipe, after the insulation test accomplished, the sample was cooled to room temperature in the furnace. During wetting process, photos were taken at a speed of two frames per second using a high-resolution (1504 × 1000 dpi) CCD camera. The contact angles and diameters of solid–liquid interface were computed by using axisymmetric drop shape analysis-profile software (ADSA-P) from shot photographs.

Three-point-bending tests were carried out to measure flexural strength of infiltrated B_4C–2519Al composites and the dimension of the bars was 35 mm × 4 mm × 3 mm with a support span of 30 mm. The flexural strength is given by the following equation:

$$\sigma_f = \frac{3FL}{2bh^2} \tag{1}$$

where F is the measured load at fracture (N), L is the support span distance (mm), b is the width of the specimen (mm), and h is the specimen thickness (mm). All tests were performed using an Instron 3369 mechanical testing machine under a crosshead speed of 0.5 mm/min. The hardness of the B_4C–2519Al composites was evaluated by the Rockwell A indentations (HRA) using a standard A indentation tester The Rockwell A diamond stylus (cone apex angle 120°, tip radius R=0.2 mm) was used to perform the tests. The applied load on the stylus was 60 kg.

After the wetting and infiltrating experiments, the selected specimens were sectioned and polished for microstructure observation using field emission scanning electron microscopy (FE-SEM) (FEI nano230) and optical microscopy (Leica, MeF3A). The bulk density and porosity were determined by the Archimedes' method and bulk chemical compositions of phases were determined by electron probe X-ray microanalysis (EPMA, JXA-8530F). The crystalline phases were characterized by X-ray diffraction (XRD) (Rigaku 3014) technique by using CuK_α radiation.

3. Results

3.1. Microstructure of boron carbide substrate

The density of B_4C substrates used in the experiment is 2.29 g/cm^3, and the sintered relative density is 91%. Fig. 1 shows the different magnifications of metallographs (Fig. 1a, b) and SEM images (Fig. 1c, d) of B_4C substrates. The specimens were both electrochemically etched using KOH dissolved in distilled water as the electrolyte. Most of the grain boundaries show bright contrast and samples are composed of equiaxed grains, which appear as straight and sharp grain boundaries. It shows a wide range of grain size extending from 6 μm to 48 μm. In addition, a low-density of crystal defects, such as twins, planar stacks were observed in the substrate.

It was well known that boron carbide has α-rhombohedral crystal structure [18–21], which is hard to slip in plastic deformation. During hot-pressing at high temperature up to 1800 °C, however, it deformed by mechanical twinning or growth twinning mode, which need higher deformation stored energy and may shear to the matrix. The nucleation and growth mechanism of these compression twins in boron carbide are not clear.

Two types of darker regions were viewed in the micrograph (Fig. 1a, b), one was large and connected holes, and the other was small stripe pores. The formation of these connected holes has not only resulted from the incomplete densification during sintering, but also due to the pull-out surface of boron carbide grain, which were left during metallographic sample preparation because of the low toughness of boron carbide. This can be recognized in the SEM images of Fig. 1c, d.

3.2. Contact angle

Fig. 2a shows the variations in contact angles with time for the molten 2519Al alloy on B_4C surfaces at 1000–1250 °C. Two representative sessile drop images at 1200 °C, which at moments of $t=0$ s and $t=1800$ s, are also shown in Fig. 2a. All the samples show a similar behavior of the contact angle versus time over the entire temperature range, and the contact angle depends on both the temperature and the time. The contact angles decreased rapidly in the initial several minutes and then approaches a steady value gradually, while the time needed to reach the steady value decreases with the increase in temperature. The initial contact angles are 111.5° (1000 °C), 103.9° (1100 °C), 79.6° (1200 °C) and 56.7° (1250 °C). The final contact angles reach 54.5° (1000 °C), 47.9° (1100 °C), 35.7° (1200 °C) and 34.5° (1250 °C) after 30 min of heat preservation.

Further analysis indicated that the temperature-dependent variation of initial contact angles at 1000–1250 °C follow an exponential decay law (Fig. 2b),

$$\theta_I = 116.94 - 0.00026 \exp(T/101.07) \quad (2)$$

where θ_I is the initial contact angle, and T is the experiment temperature. This result is different from pure Al on boron carbide, which has a linear relationship in a temperature range of 900–1200 °C [8].

The final contact angles' dependence on temperatureis described by the following linear relationship (Fig. 2b):

$$\theta_f = 141.2 - 0.086T \quad (3)$$

where T is the experiment temperature, and θ_f is the final contact angle at different temperature range.

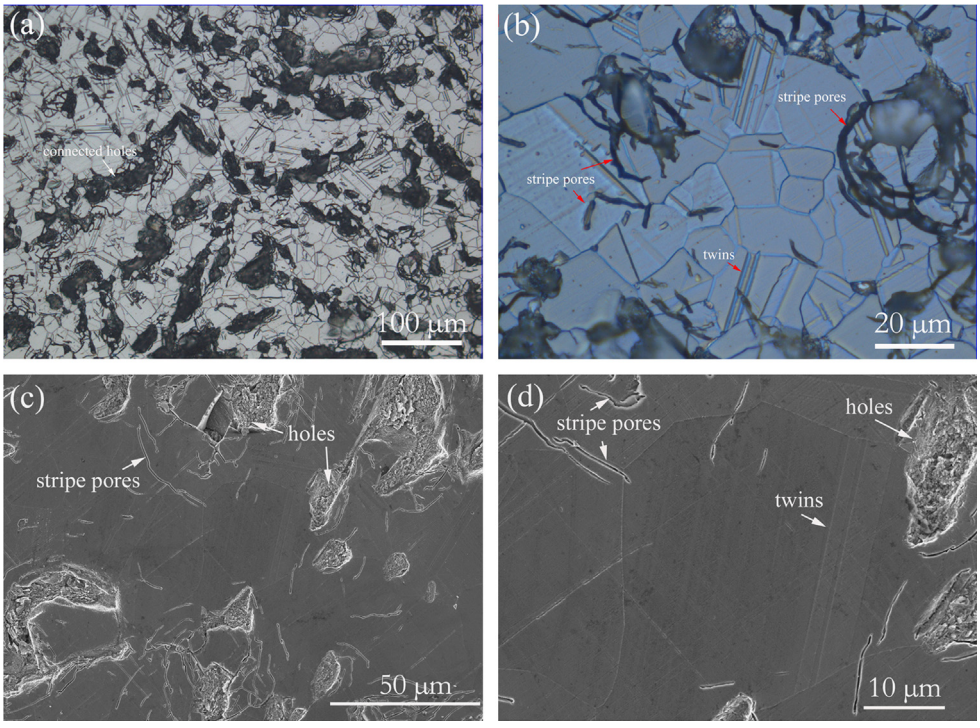

Fig. 1. Optical micrographs (a, b) and SEM images (c, d) of hot-press B_4C substrate.

As shown in Fig. 2b and Eqs. (2) and (3), the initial contact angles decrease relatively rapidly during temperature of 1000 °C–1250 °C. This may be related to the interfacial chemical reactions as well as the rupture of Al_2O_3-membrane between the molten Al and B_4C, which will be discussed in the next chapter.

3.3. Interface microstructure

Fig. 3a shows the XRD patterns of B_4C/2519Al at the surfaces of the solidified Al drops during 1000–1250 °C. It is found that a great number of Al_2Cu and Al_3Zr phases were present at the drop surface, which precipitated during cooling. A representative XRD pattern of the interface tested at 1200 °C is shown in Fig. 3b. At temperature of 1200 °C, large amounts of Al_3BC were identified. In addition, some $Al_3B_{48}C_2$, AlB_2 and Al_4C_3 compounds appeared at 1200 °C.

Fig. 4 shows the cross-sectional secondary electron images of samples wetting at 1000 °C (Fig. 4a) and 1200 °C (Fig. 4c) after 30 min. Fig. 4b and d shows enlarged region of the block in Fig. 4a and c. In combination with XRD and EDS analyses, the reaction products of Al_3BC and AlB_2 were identified in all the samples. As wetting temperature increased from 1000 °C to 1200 °C, the amount of Al_3BC phase increased. The AlB_2 phases, which have the morphology of rods or ribbon, were found to increase steadily with increasing temperature. According to the binary phase diagram of Al–Zr, the solubility of Zr in Al is close to 10 wt% in an equilibrium state of 1200 °C; therefore, the strengthening phases such θ, Al_3Zr in 2519Al will be re-dissolved into the Al liquid, and re-precipitated as coarse Al_2Cu and Al_3Zr phases during cooling.

The microstructure and phases of B_4C–2519Al samples were well revealed by the EPMA technique as shown in Fig. 5. It shows similar morphological features as those presented in Fig. 4, namely, with many boride crystals (AlB_2) grown in 2519Al drop and a rough B_4C surface covered by a layer of Al_3BC crystals (marked as "2"). Some large islands-like phases, presented at the interface (marked as "1"), were determined as $Al_3B_{48}C_2$ (β-AlB_{12}). By careful observations on the interfacial microstructures, a red layer, which has morphologies of coarse grains and are adjacent to theAl_3BC or $Al_3B_{48}C_2$ (Fig. 5b), were identified as Al_4C_3 phases (marked as "3" in Fig. 5a). It should be noted that the AlB_2

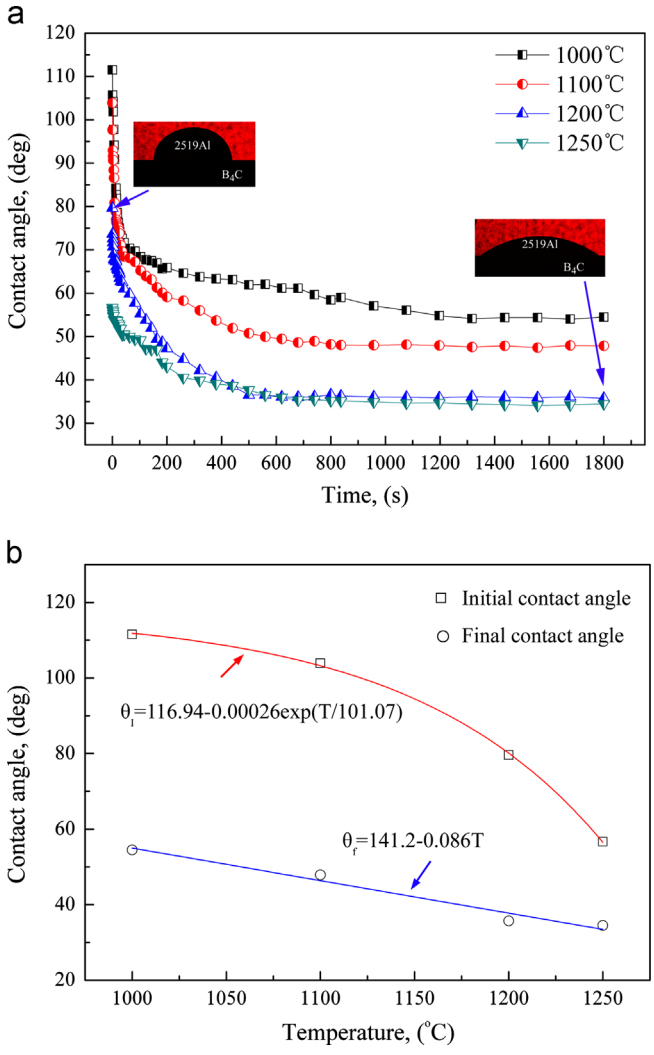

Fig. 2. (a) Variation in the contact angles with time for molten 2519Al on the B_4C substrate during 1000–1250 °C, and (b) variation in the initial and final contact angles with temperature.

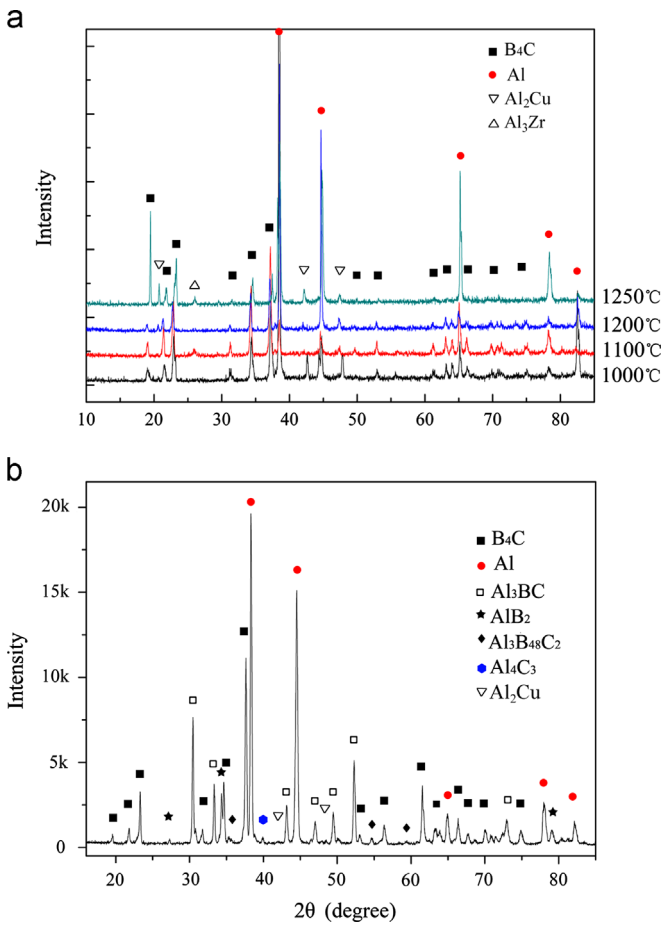

Fig. 3. XRD patterns of the B_4C–2519Al samples at the surfaces of the 2519Al drops (a) and the XRD patterns of the represented interfaces at 1200 °C (b).

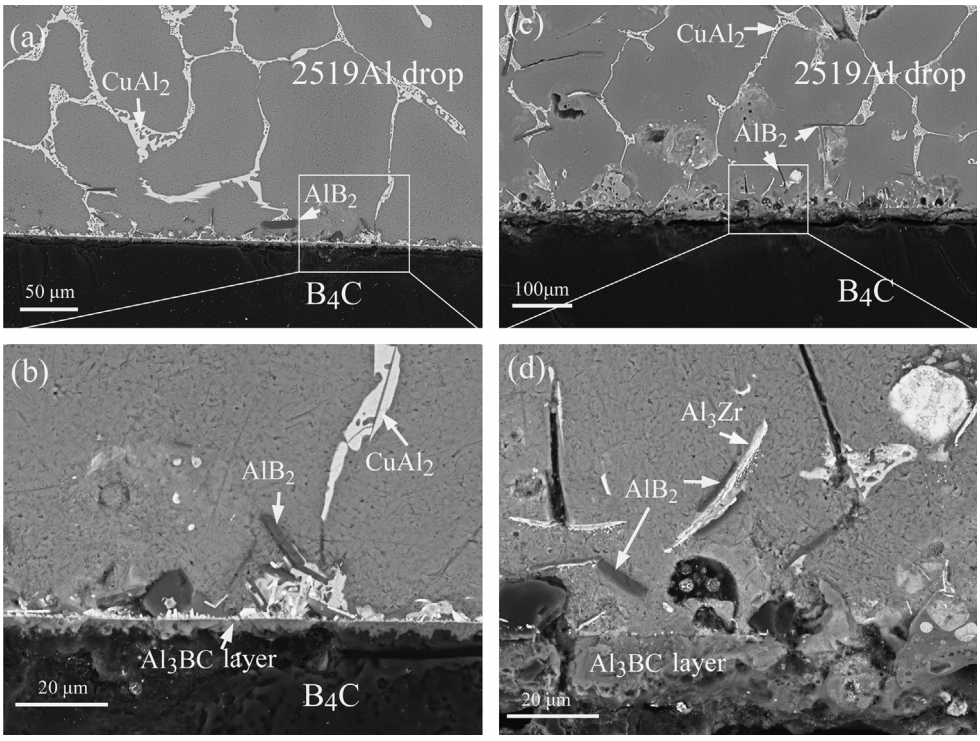

Fig. 4. SEM images of the B_4C–2519Al sample of the reaction interface with different experiment temperatures. (a, b) −1000 °C; and (c, d) −1200 °C.

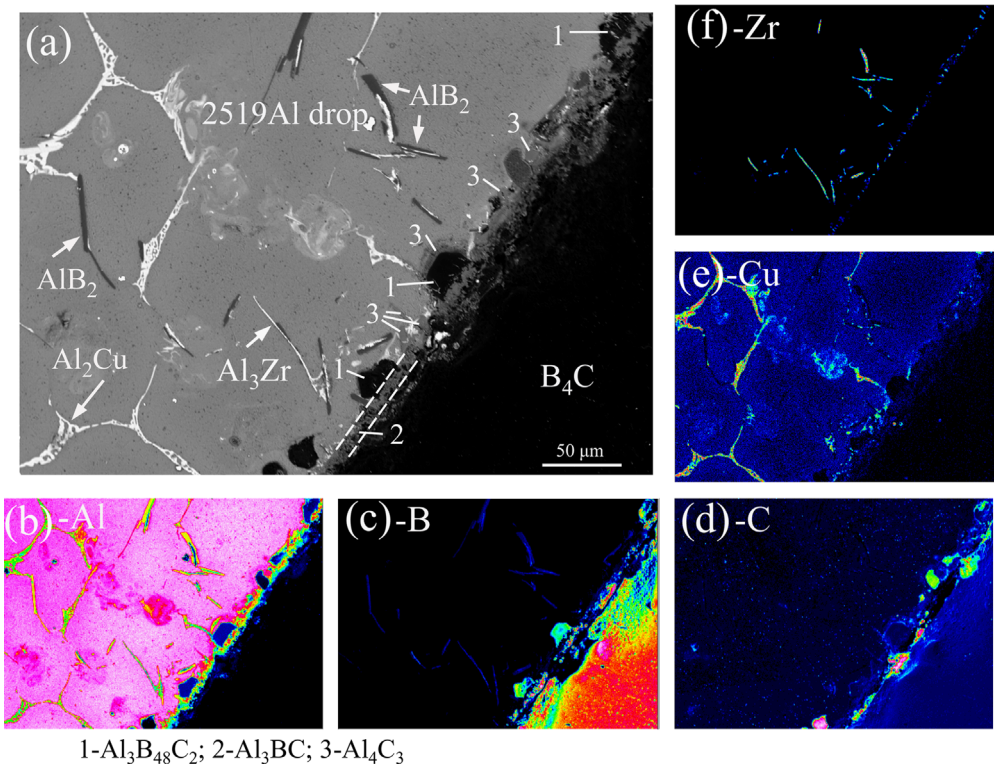

1-$Al_3B_{48}C_2$; 2-Al_3BC; 3-Al_4C_3

Fig. 5. EPMA backscattered electron micrographs near the interface of B_4C–2519Al (a) and corresponding X-ray images for respective elements: (b) aluminum, (c) boron, (d) carbon, (e) copper and (f) zirconium.

phase is unstable at temperatures higher than 950 °C because of the peritectic transformation of α-AlB_{12}+liquid → AlB_2 [22] and the boron-rich α-AlB_{12} or $Al_3B_{48}C_2$ (β-AlB_{12}) phase present at the interface at $T \geq 950$ °C, and some of it transformed to AlB_2 during cooling.

3.4. Flexural strength and hardness of typical B_4C–2519Al composites

Fig. 6 shows a typical load–displacement curve for the B_4C–2519Al composites. The density of the composite is 2.62 g/cm^3

with 0.1% porosity. It was observed that the nearly fully dense composites have only elastic deformation with little displacement, indicating brittle fracture. The average flexural strength of five samples is about 300 MPa (Table 1), which is lower than that of HP-B_4C and SPS-B_4C (~430 MPa) [1,2,31]. The average hardness of the samples is HRA 80.3 (Table 2), which is lower than pure B_4C. As shown in Fig. 7, the fracture surfaces were flat and the cracks appeared mainly in the transcrystalline form, partly in the intercrystalline form. Besides the matrix and the reinforcement, mechanical properties of ceramic–metal composites are also related to the density of complex and the interface reaction. For B_4C–Al composite, high volume fraction of boron carbide is carrying the main load. When bending load exceeds the elastic limit of boron carbide, the crack is formed at the interface and it propagated the boron carbide grains quickly, causing the composites failure. At 1200 °C infiltration process, Al_3BC phases formed along the interface between B_4C and Al, reducing the interfacial strength. As a result, the flexural strength is markedly decreased compared with pure B_4C.

4. Discussion

The effects of interface reaction on the wetting behavior of Al/B_4C and the wetting mechanism of it are still not clear or subject to controversy. Viala [10] and Arslan [12] consider that in Al/B_4C system the wetting seems to be associated with the formation of Al_3BC only. The formation of AlB_2 and AlB_{12} phases plays limited effects on wetting because B_4C particles are generally surrounded by Al_3BC crystals, while other crystals are most often embedded in the Al matrix, far away from the B_4C/Al reaction front. This result is in agreement with the work of Fujii [23] who did not detect uniformly distributed α-AlB_{12} and AlB_2 crystals throughout the BN–Al interface.

However, in view of complex compound of $Al_{2.1}B_{51}C_8$ formed at the interface, Qiaoli Lin [8] and Kharlamov [24] consider that the wettability of B_4C by pure Al was determined by the formation of different reaction products, where the Al_3BC phase makes a considerable, yet limited, contribution to the wettability (contact angle 4°at 1200 °C after 100 s). The formation of the B-rich phases, particularly $Al_{2.1}B_{51}C_8$ (or $AlB_{24}C_4$), can more significantly improve their wettability.

The formation of the Al_3BC and AlB_2 phase in the B_4C/Al was described by Viala and Bouix [10] through a classical dissolution–precipitation mechanism. The molten Al rapidly saturated in B and C by simple dissolution of the boron carbide due to very low solubility of these elements in Al, and then the Al_3BC nucleated at the surface of B_4C. The AlB_2 phases nucleated with difficulty and were only embedded in the Al matrix as shown in Figs. 3 and 5, far away from the B_4C/Al reaction front. Through the interface reaction, the liquid melt is spread out in all directions and the wetting angles decreased significantly in the first 200 s (Fig. 2a). When Al_3BC crystals tend to join together and form a dense layer of B_4C surface, the substrate is protected against further attack. At this stage, further growth of reaction product crystals may obey another

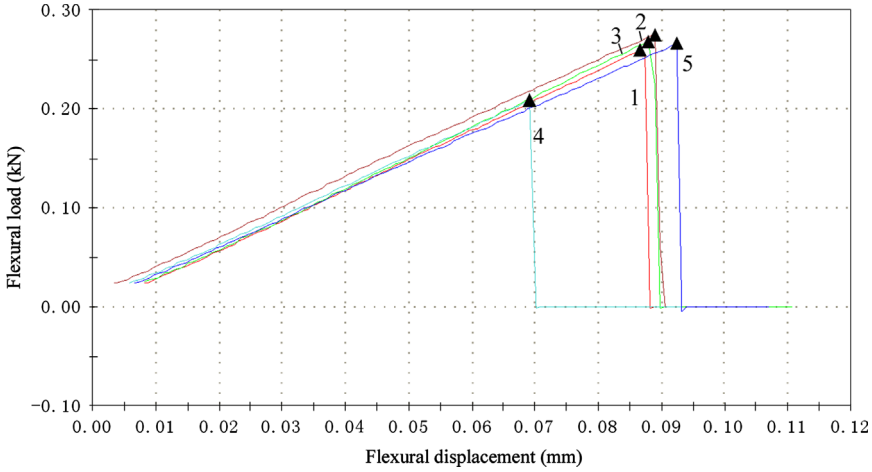

Fig. 6. The load–displacement curves for typical B_4C/2519Al composites under flexural testing.

Table 1
The flexural strength of typical infiltrated B_4C–2519Al composites.

Sample	Density (g/cm^3)	Maximum load F (N)	Bending strength σ_f (MPa)
1	2.62	258.66	301.30
2	2.62	275.06	320.40
3	2.62	268.02	330.60
4	2.62	207.86	242.12
5	2.62	265.48	309.24
Average	2.62	255.01	300.73

mechanism that implies solid-state diffusion of B, C or Al atoms through the growing Al_3BC layer. The solid-state diffusion through the Al_3BC layer has become rate controlling, where the decompose rate of B_4C decreases considerably, resulting in the wetting contact angles to have a stable value (Fig. 2a). The formation of the Al_3BC layer is temperature dependent because the dissolution and solid diffusion processes are thermally activated. Thus the spreading of melt is faster and the contact angle decreased with the increase in temperature (Fig. 2), while the final wettability does not vary significantly at $T > 1200\ ^\circ C$.

The larger contact angles at $T < 1000\ ^\circ C$ are likely to be influenced by the oxide films present at the Al and B_4C surfaces When the temperature was at $T > 1000\ ^\circ C$, a self-cleaning reaction of Al drop was formed [25]

$$4Al\ (1) + Al_2O_3(s) = 3Al_2O(g) \quad (4)$$

The exothermal reaction, which enhanced the temperature in extremely small regions, could accelerate the reaction process. This phenomenon, to a large extent, led to the fracture of Al_2O_3-membrane between the molten Al and substrate. The direct contact between Al and B_4C was extraordinarily beneficial to the progressing of the reactions on the interface and decreases the interfacial energy.

The interaction of the melt with boron carbide leads to the dissolution of boron into the melt and the concomitant release of free carbon. However, the solubility of carbon in molten aluminum is extremely limited. When in excess of its solubility limit, some free carbons reacted with aluminum and forms Al_4C_3 phases, as shown in Fig. 5. With a further increase in temperature, the Al_3BC diffusion barrier might be disrupted to a large extent by the formation of $Al_3B_{48}C_2$ phase through the following reactions [22]:

$$\alpha - AlB_{12} + Al_3BC \Leftrightarrow Al_3B_{48}C_2 + L \quad (5)$$

The aluminum dodecaboride (α-AlB_{12}) has not been identified to exist in the final microstructure. However, according to the Al–B binary phase diagram [26], α-AlB_{12} might have formed during the temperature at 1000–1250 °C. It is considered that [10] a point may be reached where the liquid Al–B solution is enriched in boron due to Al depletion such that no

Table 2
The Rockwell hardness of typical infiltrated B_4C–2519Al composites.

Point	Hardness (HRA)	Density (g/cm^3)
1	79	2.62
2	81.4	2.62
3	80.3	2.62
4	80.5	2.62
Average	80.3	2.62

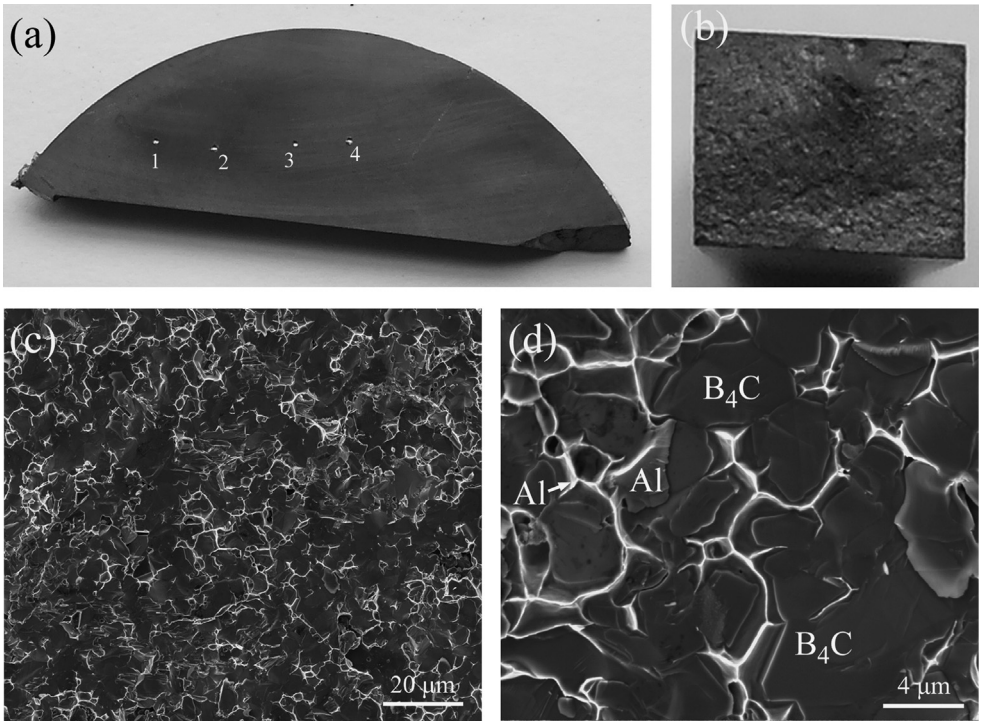

Fig. 7. The macro-morphology and microstructure of B_4C/2519Al composites, (a) typical sample after Rockwell hardness testing, (b) typical bending fracture morphology of the B_4C/2519Al sample, and corresponding fracture microstructure of the sample (c, d).

more boron can be dissolved leading to the precipitation of α-AlB_{12}. Such formed α-AlB_{12} compounds then transform to AlB_2 during cooling by a peritectic reaction [22],

$$\alpha - AlB_{12} + L \Leftrightarrow AlB_2 \quad (6)$$

It is worth mentioning that the practical reactions and phase transformations in the 2519Al–B_4C system were more complicated from 1000 °C to 1250 °C since the decomposition of the Al_3BC [22]. Moreover, Kharlamov [24] and Lin [8] suggested that boron-rich phases of $Al_{2.1}B_{51}C_8$ or $B_{13}C$ formed because the diffused rate of boron was faster than the Al in molten alloy. These boron-rich phases were broken down into several stable Al–B–C compounds, which could further expand the contact area between melt drop and B_4C substrate. Therefore, these compounds also make a great contribution to wettability.

In comparison to pure Al on B_4C [8], the final contact angles of 2519Al on B_4C have higher values of 35.7° (1200 °C) and 34.5° (1250 °C), greater than 4° for Al/B_4C at 1200 °C. This decrease of wetting behavior may be related to a copper element in the 2519Al alloy. Copper is generally regarded as non-reactive metal to B_4C, and its contact angle on B_4C ranges from 130 to 140° below 1800 °C [6,27]. Cu additions decrease the interface reaction or prohibit forming of a continuing layer of $Al_3B_{48}C_2$ and $AlB_{24}C_4$ [24], enlarge the surface tension γ_{lv} and plays a negative role on the wetting angle [28]. The equilibrium contact angle for the molten Al on the $AlB_{24}C_4$ (actually $Al_{2.1}B_{51}C_8$) phase, as reported by Kharlamov et al. [24], was 5° at 980 °C and that on the $Al_3B_{48}C_2$ phases was 12° at 1230 °C. On the other hand, the wettability of pure B by Al at 1000 °C is excellent with an equilibrium contact angle close to 0° [24] while the wettability of C or Al_4C_3 by molten Al is rather poor [29,30]. In this study, no $AlB_{24}C_4$ phases were distinguished by the EPMA and XRD techniques in the interfaces. It is reasonable to infer that the temperature dependence of the wettability of B_4C by molten 2519Al is essentially determined by the formation of different reaction products at the interface, especially the Al_3BC phase, while $Al_3B_{48}C_2$ phases makes a considerable, yet limited, contribution to the wettability. However, for pressureless infiltration fabricating the B_4C/2519Al composites, this wetting angle is enough. In actual infiltrating experiments, we found that almost full density of the B_4C/2519Al composites could be obtained at 1200 °C, which has about 35-volume percentage of 2519Al, as shown in Fig. 7.

5. Conclusion

In summary, the boron carbide substrate was prepared by hot pressing and pressureless sintering method and the wettability of B_4C by molten 2519Al at 1000–1250 °C was investigated by an improved sessile-drop method. The B_4C substrates are composed of equiaxed grains with a few crystal defects such as twins and pores. It is found that the wettability and interaction between molten 2519Al alloy and B_4C are quite sensitive to the temperature and contact time. The contact angle is significantly decreased as the temperature increased, and the minimum values, namely, 34.5° are obtained after 30 min of heat preservation at 1250 °C. When the temperature is above 1000 °C, a direct reaction between Al drop and the B_4C substrate might occur because of the rupture of Al_2O_3 film. On the other hand, the gradually growing products at interfaces, such as Al_3BC and $Al_3B_{48}C_2$, could reduce the interfacial energy between solid and liquid, which enhance the wettibility. The Al_2Cu and Al_3Zr phases appeared in 2519Al matrix during cooling after experiment, while AlB_2 precipitated far away from the interface. For infiltrated B_4C/2519Al composites, the typical bending strength and hardness are 300.71 MPa and 80.3 HRA, respectively. The main fracture way of infiltrated B_4C/2519Al is transgranular rupture, which has flat fracture surface and intrinsic brittle fracture mode.

Acknowledgments

This work was supported by the Creative Research Group of the National Natural Science Foundation of China (Grant no. 51021063) and the National Basic Research Program of China (2011CB605805).

References

[1] F. Thevenot, A review on boron carbide, Key Engineering Materials 56–57 (1991) 59–88.
[2] F. Thevenot, Boron carbide–a comprehensive review, Journal of the European Ceramic Society 6 (1990) 205–225.
[3] B.S. Lee, S. Kang, Low-temperature processing of B4C–Al composites via infiltration technique, Materials Chemistry and Physics 67 (2001) 249–255.
[4] G. de With, High temperature fracture of boron carbide: experiments and simple theoretical models, Journal of Materials Science 19 (1984) 457–466.
[5] D.C. Halverson, A.J. Pyzik, I.A. Aksay, Processing of boron carbide–aluminum composites, Journal of the American Ceramic Society 72 (1989) 775–780.
[6] J.V. Naidich, The wettability of solids by liquid metals, Progress in Surface and Membrane Science 14 (1981) 353–484.
[7] A.D. Panasyuk, V.D. Oreshkin, V.R. Maslennikova, Kinetics of the reactions of boron carbide with liquid aluminium, silicon, nickel and iron, Soviet Powder Metallurgy and Metal Ceramics 18 (7) (1979) 487–490.
[8] Qiaoli Lin, Ping Shen, Feng Qiu, Dan Zhang, Qichuan Jiang, Wetting of polycrystalline B_4C by molten Al at 1173–1473 K, Scripta Materialia 60 (2009) 960–963.
[9] M. Aizenshtein, N. Froumin, M.P. Dariel, N. Frage, Wetting and interface interactions in the B_4C/Al–Me(Me=Cu, Sn) systems, Materials Science and Engineering A 474 (2008) 214–217.
[10] J.C. Viala, J. Bouix, Chemical reactivity of aluminum with boron carbide, Journal of Materials Science 32 (1997) 4559–4573.
[11] K.B. Lee, H.S. Sim, S.Y. Cho, H. Kwon, Reaction products of Al–Mg/B_4C composite fabricated by pressureless infiltration technique, Materials Science and Engineering A 302 (2001) 227–234.
[12] Gursoy Arslan, Ferhat Kara, Servet Turan, Quantitative x-ray diffraction analysis of reactive infiltrated boron carbide–aluminium composites, Journal of the European Ceramic Society 23 (2003) 1243–1255.
[13] Xinming Zhang, Huijie Li, Hui-zhong Li, Dynamic property evaluation of aluminum alloy 2519A by split Hopkinson pressure bar, Transactions of Nonferrous Metals Society of China 18 (2008) 1–5.
[14] Huimin Wang, Changqing Xia, Pan Lei, Observation of precipitation phase in thermo-mechanical ageing 2519A aluminum alloy, Special Casting and Nonferrous Alloys 30 (11) (2010) 1040–1042.

[15] Ping Shen, Hidetoshi Fujii, Taihei Matsumot, Kiyoshi Nogi, The influence of surface structure on wetting of α-Al_2O_3 by aluminum in a reduced atmosphere, Acta Materialia 51 (2003) 4897–4906.
[16] M.W. Chen, J.W. McCauley, J.C. LaSalvia, K.J. Hemker, Microstructural characterization of commercial hot-pressed boron carbide ceramics, Journal of the American Ceramic Society 88 (7) (2005) 1935–1942.
[17] Hyukjae Lee, Robert F. Speyer, Pressureless sintering of boron carbide, Journal of the American Ceramic Society 86 (9) (2003) 1468–1473.
[18] E.M. Heian, S.K. Khalsa, J.W. Lee, Z.A. Munir, Synthesis of dense, high defect-concentration B4C through mechanical activation and field-assisted combustion, Journal of the American Ceramic Society 87 (5) (2004) 779–783.
[19] X. Fu, J. Jiang, W.Z. Zhang, J. Yuan, Incoherent structural relaxation of fivefold twinned nanowires, Applied Physics Letters 93 (4) (2008) 043101/1–043101/3.
[20] X. Fu, J. Jiang, C. Liu, J. Yuan, Five fold twinned boron carbide nanowires, Nanotechnology 20 (2009) 365707.
[21] R. Lazzari, N. Vast, J.M. Besson, S. Baroni, C.A. Dal, Atomic structure and vibrational properties of icosahedral B4C boron carbide, Physical Review Letters 83 (1999) 3230–3233.
[22] A. Grytsiv, P. Rogl, Light Metal Systems Part 1, in: G. Effenberg, S. Ilyenko (Eds.), Landolt-Börnstein–Group IV Physical Chemistry, 11A1, Springer Verlag, Berlin, 2004, pp. 29–51.
[23] H. Fujii, H. Nakae, K. Okada, Interfacial reaction wetting in the boron nitride/molten aluminum system, Acta Metallurgica Materialia 41 (10) (1993) 2963–2971.
[24] A.I. Kharlamov, S.V. Loichenko, V.I. Nizhenko, N.V Kirillova, L.I. Floka, Wetting of hot-pressed aluminum borides and borocarbides by molten aluminum and copper, Powder Metallurgy and Metal Ceramics 40 (1–2) (2001) 65–70.
[25] Jinkwan Jung, Shinhoo Kang, Advances in manufacturing boron carbide–aluminum composites, Journal of the American Ceramic Society 87 (1) (2004) 47–54.
[26] H. Duschanek, P. Rogl, The Al–B (aluminum–boron) system, Journal of Phase Equilibria 15 (5) (1994) 543–552.
[27] A.R. Kennedy, J.d. Wood, B.M. Weager, The wetting and spontaneous infiltration of ceramics by molten copper, Journal of Materials Science 35 (2000) 2909–2912.
[28] N. Froumin, N. Frage, M. Aizenshtein, Ceramic–metal interaction and wetting phenomena in the B4C/Cu system, Journal of the European Ceramic Society 23 (2003) 2821–2828.
[29] K. Landry, S. Kalogeropoulou, N. Eustathopoulos, Wettability of carbon by aluminum and aluminum alloys, Materials Science and Engineering A 254 (1–2) (1998) 99–111.
[30] A.C. Ferro, B. Derby, Wetting behaviour in the Al–Si/SiC system: interface reactions and solubility effects, Acta Metallurgica et Materialia 43 (8) (1995) 3061–3073.
[31] S. Hayuna, V. Paris, M.P. Dariel, N. Frage, E. Zaretzky, Static and dynamic mechanical properties of boron carbide processed by spark plasma sintering, Journal of the European Ceramic Society 29 (2009) 3395–3400.